JACS
JOURNAL OF THE AMERICAN CHEMICAL SOCIETY

Communication

pubs.acs.org/JACS

Temporal Control of Aptamer Biosensors Using Covalent Self-Caging To Shift Equilibrium

Zhesen Tan, Trevor A. Feagin, and Jennifer M. Heemstra*

Department of Chemistry and the Center for Cell and Genome Science, University of Utah, Salt Lake City, Utah 84112, United States

Supporting Information

ABSTRACT: Aptamer-based sensors provide a versatile and effective platform for the detection of chemical and biological targets. These sensors have been optimized to function in multiple formats, however, a remaining limitation is the inability to achieve temporal control over their sensing function. To overcome this challenge, we took inspiration from nature's ability to temporally control the activity of enzymes and protein receptors through covalent self-caging. We applied this strategy to structure-switching aptamer sensors through the installation of a cleavable linker between the two DNA fragments that comprise the sensor. Analogous to self-caged proteins, installation of this linker shifts the equilibrium of the aptamer sensor to disfavor target binding. However, activity can be restored in a time-resolved manner by cleavage of the linker. To demonstrate this principle, we chose a photocleavable linker and found that installation of the linker eliminates target binding, even at high target concentrations. However, upon irradiation with 365 nm light, sensor activity is restored with response kinetics that mirror those of the linker cleavage reaction. A key benefit of our approach is generality, which is demonstrated by grafting the photocleavable linker onto a different aptamer sensor and showing that an analogous level of temporal control can be achieved for sensing of the new target molecule. These results demonstrate that nature's self-caging approach can be effectively applied to non-natural receptors to provide precise temporal control over function. We envision that this will be of especially high utility for deploying aptamer sensors in biological environments.

Biosensors are powerful in their ability to harness the molecular recognition properties of biomolecules and use these in combination with a transduction element to enable the sensitive and specific quantification of target molecules of interest. Antibodies are frequently employed as the recognition element in biosensors, but nucleic acid aptamers have emerged over the past 25 years as a promising alternative to antibodies.[1] Aptamers are short oligonucleotides that can be generated using an *in vitro* selection process termed systematic evolution of ligands via exponential enrichment (SELEX).[2,3] Similar to antibodies, aptamers can bind to a wide variety of small-molecule and protein targets with high affinity and specificity. However, the stability of aptamers greatly exceeds that of antibodies, as aptamers can withstand thermal cycling and can function in the presence of high concentrations of surfactants.[4] An additional key benefit of aptamers is that they can be chemically synthesized having a diverse array of modifications such as fluorophores or non-native linkers. This has enabled the engineering of aptamers into a variety of biosensor formats that have found wide utility in analytical applications. Among the most popular of these is the structure-switching (SS) biosensor,[5] in which a short complementary strand is hybridized to the aptamer via Watson−Crick base pairing. Upon addition of the target molecule, the aptamer binds to the target, displacing the complementary strand. If the aptamer and displacement strand are labeled with a fluorophore and quencher, this displacement event generates a dose-dependent fluorescence signal that can be used to quantify the target molecule.

Recognizing the functional similarity between aptamers and naturally occurring proteins, Plaxco and Ricci recently published a series of reports elegantly demonstrating that biological principles such as allostery,[6] cooperativity,[7] and inhibition[8] can be used to fine-tune thermodynamic parameters including the dynamic range and overall sensitivity of aptamer-based sensors. Inspired by these reports, we envisioned that biological principles could also be used to achieve temporal control over aptamer-based sensors. Specifically, nature employs covalent self-caging to control enzyme and receptor activity in the cases of zymogens[9] and protease-activated receptors,[10] respectively. In these biological motifs, a portion of the peptide sequence serves as an inhibitor for the enzyme or receptor, and only after cleavage by a protease or other stimulus does the biomolecule gain activity. Covalent self-caging has also been successfully extended to small-molecules to enable stimuli-responsive drug delivery and activation.[11,12] To apply this concept to aptamers, we recognized that SS biosensors rely on a balance of equilibria in which the complementary strand and the target molecule compete for binding to the aptamer.[5] We hypothesized that installation of a cleavable hairpin loop[13] between the aptamer and complementary strand would temporarily shift this equilibrium to favor binding to the complementary strand, rendering the sensor functionally inert to the target molecule. However, upon cleavage of the linker, the initial equilibrium would be restored to enable dose-dependent displacement of the complementary strand in the presence of the target molecule (Figure 1).

Received: January 26, 2016
Published: May 9, 2016

DOI: 10.1021/jacs.6b00934
J. Am. Chem. Soc. 2016, 138, 6328−6331

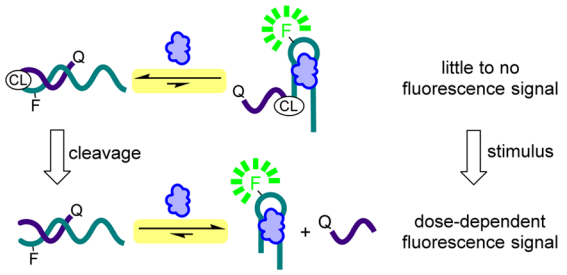

Figure 1. Installation of a cleavable linker temporarily shifts the equilibrium of the biosensor to disfavor target binding. Cleavage of the linker reverses this equilibrium shift, restoring the ability of the biosensor to bind to the target molecule and generate a dose-dependent fluorescent signal. F = fluorophore, Q = quencher, CL = cleavable linker.

We envision that the ability to achieve time-resolved control over SS biosensor activity will be of especially high utility for live cell imaging experiments, as these protocols typically require transfection of the biosensors into the cells, and this process can temporarily disrupt cellular function. Thus, to gain accurate insight into intracellular conditions, it is ideal to temporally separate the biosensing event from the transfection event. Without caging, significant background signal would likely accumulate during this delay period due to kinetic trapping of target-bound sensors. However, our caging approach will prevent this accumulation of background signal by rendering the biosensors temporarily inert to the target molecule. As an additional benefit, covalent tethering ensures that a defined stoichiometry between the aptamer and complementary strand is maintained through manipulation steps such as transfection. Given these advantages, we envision that our self-caging motif will provide the necessary control to accurately quantify intracellular targets of interest at specified time points.

For our initial demonstration of this concept, we chose a photolabile linker to form the hairpin loop. Light is often used as an external stimulus for controlling biological systems, due to its bioorthogonality and noninvasiveness.[14] Additionally, light can be manipulated both spatially and temporally, allowing for precise regulation of biosensor activity. Photolabile caging groups have been used to control the activity of aptamers[15] and nucleic acid enzymes,[16−18] but in these previous reports, the caging groups were placed on nucleotides that play key roles in binding or catalysis. In the case of nucleic acid enzymes, where the active site residues are often predetermined, this approach is highly effective. However, nucleotide caging is more challenging in the case of aptamers, as the binding site must be elucidated prior to designing the caged sequence. This process must then be repeated for each new aptamer sequence, limiting the generalizability of this method. In contrast, our approach enables efficient photoresponsive control over biosensor activity without any modifications to the nucleotide sequence of the biosensor. This obviates the need for elucidation of the key functional residues and enables our approach to be rapidly applied to aptamer biosensors for a variety of target molecules. Additionally, our approach only requires a linker containing a stimuli-responsive functional group, and thus we envision that this method will be easily adaptable to generate caged biosensors that respond to a broad range of stimuli.

To explore the effect of covalent self-caging on biosensor equilibrium, we utilized the SS biosensor for L-tyrosinamide (L-Tym), which was developed by the Peyrin lab[19] using a DNA aptamer reported by Gatto et al.[20] We demonstrate that the presence of the photocleavable hairpin dramatically shifts the equilibrium for binding of the aptamer to the complementary strand, such that no displacement is observed even at high concentrations of the small-molecule target. Upon irradiation with 365 nm light, the hairpin is cleaved, and the dose-responsive fluorescence signal of the biosensor is restored. Moreover, we show that the evolution of fluorescence signal is closely related to the kinetics of hairpin cleavage, demonstrating a high level of temporal control over biosensor activity. To demonstrate the generality of our approach, we grafted the same photolabile hairpin onto the SS biosensor for ochratoxin A[21] (OTA) and achieved an analogous level of temporal control. Together, this research demonstrates that nature's approach to achieving time-resolved control of function via covalent self-caging can be extended to biomolecules having non-native functions.

This SS biosensor for L-Tym was initially designed to utilize fluorescence polarization as the functional output, but was adapted by our lab into an intensity-based fluorescence sensor by labeling the termini of the aptamer and complementary strand with fluorescein (FAM) and black hole quencher 1 (BHQ1), respectively.[22] In our previous report, we optimized the sequence of the SS biosensor for use in the fluorophore-quencher format, but there remained a 10 nucleotide (nt) overhang on the 5′ terminus of the aptamer strand, extending beyond the annealed complementary strand. While this was not problematic in our earlier studies, we recognized that the presence of these overhanging nucleotides would erode the effectiveness of our equilibrium shifting approach, as the hairpin connecting the two strands would be much larger than necessary. Thus, we tested a truncated version of the aptamer in which these 10 nt were deleted and, fortuitously, found that this did not impact the ability of the biosensor to bind to L-Tym.

We next turned to exploring the magnitude of equilibrium shifting as a function of linker length. As mentioned above, if the linker is too long, this compromises the gain in effective molarity that is achieved by tethering of the nucleic acids. However, if the linker is too short to accommodate the diameter of the DNA duplex, this could interfere with hybridization of the two sequences and reduce the magnitude of the equilibrium shift. To explore these parameters, we synthesized four biosensor sequences in which the aptamer was tethered to the complementary strand using a photocleavable spacer (PC spacer) and a varying number of triethylene glycol (PEG_3) spacer units (Figure 2). The PC spacer we utilized contains an

Figure 2. Structure of self-caged biosensor for L-Tym. FAM = fluorescein, BHQ1 = black hole quencher 1.

ortho-nitrobenzyl group, which is cleaved by UV light at 365 nm. To assess the impact of the different linkers, we measured the melting temperature of each duplex in both the uncleaved and cleaved states. This was accomplished by monitoring temperature-dependent hyperchromicity at 260 nm. As shown in Table 1, we found that the sequence having a single PEG_3 unit in the

DOI: 10.1021/jacs.6b00934
J. Am. Chem. Soc. 2016, 138, 6328−6331

Table 1. Melting Temperature (T_m) of L-Tym Biosensor As a Function of Linker Length and Cleavage State[a]

sequence	n	T_m (uncleaved, °C)	T_m (cleaved, °C)	ΔT_m (°C)
TA-0S	0	72.4 ± 0.4	35.3 ± 0.6	37.1
TA-1S	1	78.1 ± 1.6	35.3 ± 0.6	42.8
TA-2S	2	69.2 ± 3.4	34.0 ± 0.9	35.2
TA-3S	3	70.0 ± 2.6	35.3 ± 1.0	34.7

[a]Errors represent the standard deviation of three independent trials.

linker (TA-1S) showed the greatest change in duplex stability, with the presence of the hairpin increasing T_m by 42.8 °C. To quantify the magnitude of equilibrium shifting provided by the linker, we utilized van 't Hoff analysis to obtain thermodynamic parameters for each duplex (Table S4).[23] A $\Delta\Delta G^\circ$ value of 18.0 kJ/mol was calculated for cleaved vs uncleaved TA-1S, representing a 1400-fold change in equilibrium constant. The T_m and $\Delta\Delta G^\circ$ values for the other sequences also supported our hypotheses regarding linker length, as sequences having linkers that are too short (TA-0S) or longer than necessary (TA-2S and TA-3S) form less stable duplexes compared to TA-1S. As anticipated, the T_m values for the cleaved sensors are independent of linker length. Given these data, we chose to use linkers having one PEG_3 unit in all subsequent experiments.

Encouraged by the large impact of the linker on duplex stability, we turned to investigating the kinetics for linker cleavage. Sequence TA-1S was irradiated for varying amounts of time using a UV transilluminator, then analyzed using denaturing polyacrylamide gel electrophoresis (PAGE). Staining with SYBR Green II followed by fluorescence imaging enabled quantification of cleavage yield as a function of time (Figure 3). These data were fit to a first order kinetic model to provide a rate constant (k) of 1.36×10^{-3} s^{-1} and a half-life ($t_{1/2}$) of 8.5 min (Figure S4).

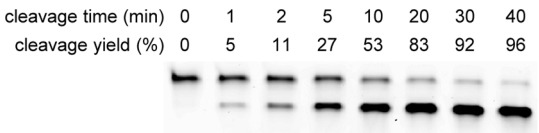

Figure 3. Photocleavage of L-Tym biosensor was examined using denaturing PAGE to quantify kinetics for the uncaging reaction.

Having optimized the linker length and quantified cleavage kinetics, we next turned to exploring the effectiveness of our covalent self-caging approach. This was accomplished by irradiating the TA-1S biosensor at 365 nm for varying lengths of time, ranging from 0 to 20 min. The samples were then transferred to a 384-well plate and incubated with varying concentrations of L-Tym for 20 min at 25 °C. This relatively long incubation time was employed to ensure that the solutions reached equilibrium, such that any effect from the presence of the linker could be attributed to equilibrium shifting, as opposed to kinetic trapping. Fluorescence intensity was then measured and used to calculate percent displacement, defined as the percentage of biosensors having the complementary strand dehybridized from the aptamer.[22] Excitingly, Figure 4a shows that the fully caged TA-1S sensor (0 min, dark-blue circles) provides no target response, even at high L-Tym concentrations. This suggests that the presence of the linker provides a sufficient shift in equilibrium to completely deactivate the sensor. We were also encouraged by the effectiveness of the uncaging process, as sensors that were cleaved with UV light showed

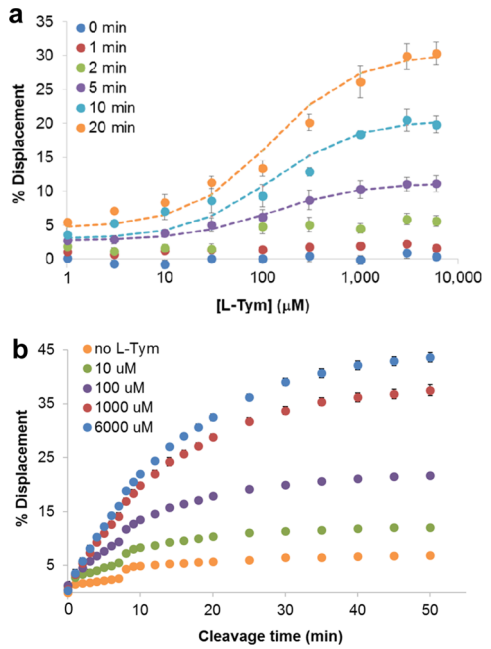

Figure 4. (a) Dose-dependent response of L-Tym biosensor (TA-1S) as a function of cleavage time. Error bars represent the standard deviation of three independent trials. Dashed lines represent fitting to a Langmuir isotherm. (b) Real-time monitoring of biosensor response upon uncaging in the presence of varying concentrations of L-Tym. [TA-1S] = 1 μM in 10 mM Tris-HCl, 100 mM NaCl, 5 mM KCl, 2 mM $MgCl_2$, 1 mM $CaCl_2$, pH 7.5. All fluorescence data are normalized to reflect % displacement of the complementary strand from the aptamer.

dose-dependent displacement. We also observe that the overall magnitude of the dose-dependent displacement increases with increasing irradiation time. This is to be expected, as longer irradiation times produce higher concentrations of uncaged sensors. The dose–response curves for the three longest irradiation times were each fit to a Langmuir isotherm and reveal that the affinity of the sensor for the target does not change significantly as a function of cleavage time and is comparable to the previously reported target affinity for this sensor[22] (Table S7). Interestingly, even when the sensor is fully cleaved, we do not observe full displacement of the complementary strand at high target concentrations. We have previously observed this phenomenon for multiple SS biosensors[4,22] and hypothesize that this is the result of accumulation of complementary strand as displacement occurs, which then serves as an inhibitor to further displacement events.

While our initial experiments used a 20 min incubation time to ensure that the biosensors reached equilibrium, we recognized that this is not practical for our desired application of time-resolved biosensor activation. Thus, we conducted an additional experiment to evaluate the ability of the biosensor to generate target-dependent signal in real-time as the uncaging occurs. For this experiment, uncleaved TA-1S was combined with varying concentrations of L-Tym, and the reaction mixture was irradiated with 365 nm light. Fluorescence intensity was measured at specific time points to reflect the real-time response of the sensor, and these data are plotted in Figure 4b. An overlay of the kinetics data from our linker cleavage experiment revealed a close correlation with the time-dependent biosensor signal (Figure S7). This indicates that the biosensor is able to rapidly re-establish equilibrium after uncaging, providing a high level of temporal control over sensing of target analytes.

DOI: 10.1021/jacs.6b00934
J. Am. Chem. Soc. 2016, 138, 6328–6331

As discussed earlier, a key benefit of our equilibrium-shifting approach is that it does not require direct modification of the target binding site. Thus, it is likely to be generally applicable to SS biosensors for a wide variety of targets. To explore this possibility, we utilized the DNA SS biosensor for OTA[21] and grafted the PC spacer-PEG_3 linker from TA-1S onto this new biosensor architecture. We also incorporated FAM and BHQ1 labels at similar positions to those in TA-1S (see Supporting Information). The OTA biosensor is known to provide ideal signal background in the presence of an excess of complementary strand. Thus, we added 2 equiv of BHQ1-labeled complementary strand (OA-CS) to all of the OA-1S samples. We repeated our experiment measuring target-dependent fluorescence signal as a function of cleavage time (Figure 5)

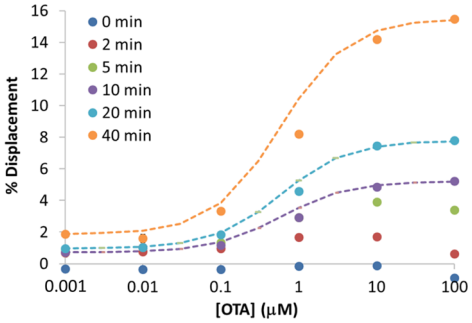

Figure 5. Dose-dependent response of OTA biosensor (OA-1S) as a function of cleavage time. Dashed lines represent fitting to a Langmuir isotherm. Error bars represent the standard deviation of three independent trials. [OA-1S] = 45 nM in 10 mM Tris-HCl, 120 mM NaCl, 5 mM KCl, 1 mM $CaCl_2$, 90 nM OA-CS, pH 8.5. All fluorescence data are normalized to reflect % displacement of the complementary strand from the aptamer.

and found that our results mirrored those obtained for the L-Tym biosensor, with no signal observed prior to cleavage, and an increase in dose-dependent signal intensity with increasing cleavage time. Fitting of these data to a Langmuir isotherm showed that the affinity of the sensor for the target remains constant across the three highest cleavage times (Table S12). We also repeated the real-time sensing experiment with the OA-1S biosensor and found that we can achieve time-resolved sensing of different OTA concentrations (Figure S8).

In summary, we show that nature's covalent self-caging strategy can be applied to non-natural receptors as a novel method for achieving temporal control over the activity of SS aptamer biosensors. Specifically, we found that installing a photocleavable linker between the aptamer and complementary strand results in a 1400-fold increase in equilibrium constant for binding of the aptamer to the complementary strand. This renders the biosensor inert to the target molecule, but activity can be restored in a time-resolved manner by cleaving the hairpin loop using UV light, after which dose-dependent fluorescence signal is observed. A key benefit to our self-caging approach is that no modifications to the nucleotide sequence of the biosensor are required, and we demonstrate that the cleavable linker can be easily grafted onto a different SS biosensor to provide similar time-resolved control over biosensor activity. Thus, our equilibrium shifting approach provides a generalizable method for achieving temporal control over target detection. We anticipate that this will be especially beneficial for biological applications, where biosensor delivery and the desired time frame for sensing are not necessarily aligned. Future experiments will be aimed at exploring additional linker-stimuli pairs and deploying our caged sensors in complex biological environments.

■ ASSOCIATED CONTENT

Supporting Information

The Supporting Information is available free of charge on the ACS Publications website at DOI: 10.1021/jacs.6b00934.

Experimental details and data (PDF)

■ AUTHOR INFORMATION

Corresponding Author

*heemstra@chem.utah.edu

Notes

The authors declare no competing financial interest.

■ ACKNOWLEDGMENTS

This work was supported by the National Science Foundation (CHE 1308364 to J.M.H.).

■ REFERENCES

(1) Liu, J.; Cao, Z.; Lu, Y. *Chem. Rev.* **2009**, *109*, 1948.
(2) Ellington, A. D.; Szostak, J. W. *Nature* **1990**, *346*, 818.
(3) Tuerk, C.; Gold, L. *Science* **1990**, *249*, 505.
(4) Peterson, A. M.; Jahnke, F. M.; Heemstra, J. M. *Langmuir* **2015**, *31*, 11769.
(5) Nutiu, R.; Li, Y. *J. Am. Chem. Soc.* **2003**, *125*, 4771.
(6) Simon, A. J.; Vallée-Bélisle, A.; Ricci, F.; Plaxco, K. W. *Proc. Natl. Acad. Sci. U. S. A.* **2014**, *111*, 15048.
(7) Simon, A. J.; Vallée-Bélisle, A.; Ricci, F.; Plaxco, K. W. *Angew. Chem., Int. Ed.* **2014**, *53*, 9471.
(8) Porchetta, A.; Vallée-Bélisle, A.; Plaxco, K. W.; Ricci, F. *J. Am. Chem. Soc.* **2012**, *134*, 20601.
(9) Nelson, D. L.; Cox, M. M. *Lehninger Principles of Biochemistry*; 3rd ed.; Worth Publishers: New York, 2000.
(10) Saito, T.; Bunnett, N. W. *NeuroMol. Med.* **2005**, *7*, 79.
(11) Zindler, M.; Pinchuk, B.; Renn, C.; Horbert, R.; Dobber, A.; Peifer, C. *ChemMedChem* **2015**, *10*, 1335.
(12) Choi, K. Y.; Swierczewska, M.; Lee, S.; Chen, X. *Theranostics* **2012**, *2*, 156.
(13) Tang, X.; Dmochowski, I. J. *Angew. Chem., Int. Ed.* **2006**, *45*, 3523.
(14) Riggsbee, C. W.; Deiters, A. *Trends Biotechnol.* **2010**, *28*, 468.
(15) Heckel, A.; Mayer, G. *J. Am. Chem. Soc.* **2005**, *127*, 822.
(16) Lusic, H.; Young, D. D.; Lively, M. O.; Deiters, A. *Org. Lett.* **2007**, *9*, 1903.
(17) Ting, R.; Lermer, L.; Perrin, D. M. *J. Am. Chem. Soc.* **2004**, *126*, 12720.
(18) Hwang, K.; Wu, P.; Kim, T.; Lei, L.; Tian, S.; Wang, Y.; Lu, Y. *Angew. Chem., Int. Ed.* **2014**, *53*, 13798.
(19) Zhu, Z.; Schmidt, T.; Mahrous, M.; Guieu, V.; Perrier, S.; Ravelet, C.; Peyrin, E. *Anal. Chim. Acta* **2011**, *707*, 191.
(20) Vianini, E.; Palumbo, M.; Gatto, B. *Bioorg. Med. Chem.* **2001**, *9*, 2543.
(21) Chen, J.; Fang, Z.; Liu, J.; Zeng, L. *Food Control* **2012**, *25*, 555.
(22) Feagin, T. A.; Olsen, D. P. V.; Headman, Z. C.; Heemstra, J. M. *J. Am. Chem. Soc.* **2015**, *137*, 4198.
(23) Marky, L. A.; Breslauer, K. J. *Biopolymers* **1987**, *26*, 1601.

DOI: 10.1021/jacs.6b00934
J. Am. Chem. Soc. 2016, 138, 6328−6331